Nitroaromatic explosives detection by a luminescent Cd(II) based metal organic framework

Dear author,

Please note that changes made in the online proofing system will be added to the article before publication but are not reflected in this PDF.

We also ask that this file not be used for submitting corrections.

Polyhedron xxx (2016) xxx–xxx

Contents lists available at ScienceDirect

Polyhedron

journal homepage: www.elsevier.com/locate/poly

Nitroaromatic explosives detection by a luminescent Cd(II) based metal organic framework

Shibashis Halder [a], Pritam Ghosh [b], Corrado Rizzoli [c], Priyabrata Banerjee [b,d], Partha Roy [a,*]

[a] Department of Chemistry, Jadavpur University, Jadavpur, Kolkata 700 032, India
[b] Surface Engineering & Tribology Group, CSIR-Central Mechanical Engineering Research Institute, Mahatma Gandhi Avenue, Durgapur 713209, West Bengal, India
[c] Universita' degli Studi di Parma, Dipartimento di Chimica, Parco Area delle Scienze 17/A, I-43124 Parma, Italy
[d] Academy of Scientific & Innovative Research (AcSIR) at CSIR-CMERI, Mahatma Gandhi Avenue, Durgapur 713209, West Bengal, India

ARTICLE INFO

Article history:
Received 18 October 2016
Accepted 25 November 2016
Available online xxxx

Keywords:
Cd-based MOF
Nitroaromatics
Fluorescence
Quenching
DFT

ABSTRACT

A Cd(II) based coordination polymer, $[Cd(3\text{-bpd})(N(CN)_2)_2]_n$ (**1**), where 3-bpd is 1,4-bis(3-pyridyl)-2, 3-diaza-1,3-butadiene, has been synthesized and characterized by standard methods including single crystal X-ray diffraction technique. Singly crystal X-ray diffraction analysis shows that it is a 3-dimensional metallo-organic framework. **1** exhibits strong emission intensity in dispersed acetonitrile at 430 nm when it is excited at 340 nm. Among different explosive and pollutant nitroaromatic compounds (epNACs), trinitrophenol (TNP) is able to quench emission intensity of **1** drastically making **1** as turn-off chemosensor for TNP. Other epNACs, e.g. 2,4,6-trinitrotoluene (TNT), 2,6-dinitro toluene (2,6-DNT), nitrobenzene (NB), 1,3-dinitro benzene (1,3-DNB), 3,4-dinitrotoluene (3,4-DNT) and 4-nitrobenzoic acid (4-NBA) cannot quench the emission intensity of **1** significantly. The quenching constant value of **1** for TNP is determined to be $7.16 \times 10^4\ M^{-1}$. Limit of detection of the complex towards TNP is 6×10^{-5} M. Resonance energy transfer (RET) is involved in the transfer of energy from the electronically excited donor, **1** to the acceptor, TNP thereby quenching the emission intensity. Some theoretical calculations have been performed to support the electronic transitions and the proposed mechanism.

1. Introduction

Metal–organic frameworks (MOFs), which are also known as porous coordination polymers (PCPs), are a class of porous materials. These are built from metal containing nodes and organic/inorganic linkers [1]. MOFs are in ever increasing interesting research area because of their structural diversities and their potential applications in many fields of scientific research e.g. gas storage and removal [2], catalysis [3], electronic devices [4], sensing [5], magnetism [6] etc. MOFs can be synthesized by the choice of metal center, organic ligand and bridging moiety under suitable reaction conditions. During synthesis of an MOF, one has to be conscious about the reaction conditions. Due to the presence of several reactants in the reaction medium, control of the reaction is highly important to get desired product which can successfully achieve the required application. Temperature, pressure, solvent, counter anion of the metal salt etc. play very crucial role to design different MOFs with various dimensionalities.

On the other hand several nitroaromatic compounds quench the emission intensity of MOFs. This property of MOF can be used to detect explosive and pollutant nitro aromatic (epNAC) compounds. In recent time terrorist activity is a global challenge. Terrorist attack in different part of world occupies to the news headlines almost every week. It is important to develop suitable system that can readily recognize the explosives in order to improve homeland security and restrict terrorist activities. Example of epNACs includes 2,4,6-trinitrotoluene (TNT), 2,6-DNT (2,6-dinitro toluene), NB (nitro benzene), 1,3-DNB (1,3-dinitro benzene), 3,4-DNT (3,4-dinitro toluene), 4-nitrobenzoic acid (4-NBA) and 2,4,6-trinitrophenol (TNP, also known as picric acid) etc. These compounds are often used as explosives or to prepare explosives and some of them are themselves highly explosive.

In recent years several articles have been published related to the sensing of TNT by MOFs but very little attention has been reserved to the detection of 2,4,6-trinitrophenol which is even more powerful than TNT as an explosive [7]. Apart from this, TNP can be used in dyes and fireworks, pharmaceutical industries, staining material, glasses, analytical chemicals [8], etc. When discharged into the environment it can pollute ground water and soil [9,10] potentially creating several health issues such as anemia,

* Corresponding author. Fax: +91 3324146414.
E-mail address: proy@chemistry.jdvu.ac.in (P. Roy).

http://dx.doi.org/10.1016/j.poly.2016.11.039
0277-5387/

infertility, respiratory track, carcinogenesis inside human cells and other living organisms [11,12], etc. Hence, detection of picric acid is an important issue considering its role as both explosive and pollutant.

MOFs constructed by d^{10} metal ions and aromatic π-conjugated ligands are supposed to be promising candidates to perform as photoactive materials [13–18]. For these reasons, luminescent properties of several MOFs with such constituents have been explored. MOFs with Cd, Zn metal ions have been reported as sensors for nitroaromatic compounds. Mukherjee et al. have developed Zn-based MOFs with electron rich aromatic ligands or ligands with fluorophore for sensing of explosives [19,20]. Luminescent Zn-based MOFs with electron rich organic ligand have been used for the sensing of TNP [21,22]. A recent report shows the use of Zn-based MOF constructed from π-conjugated thiophene-containing carboxylic acid as ligand for the detection of nitroaromatics [23].

In this connection, we report here the synthesis, characterization and TNP sensing properties of a Cd(II) based MOF, $[Cd(3\text{-bpd})(N(CN)_2)_2]_n$ (**1**) where 3-bpd is 1,4-bis(3-pyridyl)-2,3-diaza-1,3-butadiene. **1** was prepared under ambient reaction conditions and characterized by standard techniques including X-ray single crystal diffraction analysis. 3-bpd was selected because its π-conjugated system is fluorescent, it is an electron rich ligand with good delocalization, and the rotation about the N–N bond of the two pyridyl units can regulate the coordination orientation of the binding atoms. Coordination polymers with bpd ligand also show promising fluorescence properties [24]. This encouraged us to explore the fluorescence properties of **1** towards sensing the electron deficient nitroaromatic compounds.

2. Experimental

2.1. Materials and physical methods

Pyridine-3-carboxaldehyde and hydrazine hydrate were purchased from Aldrich Chemical Co. and were used as received. $Cd(NO_3)_2{\cdot}4H_2O$ was purchased from Merck, India. 1,4-Bis(3-pyridyl)-2,3-diaza-1,3-butadiene(3-bpd) was synthesized following the procedure reported earlier [24a]. All the other chemicals including solvents were of reagent grade and were used as received without further purification. 2,4,6-Trinitrotoluene (TNT) was prepared by the synthesis procedure reported in the literature [25]. Elemental analyses (carbon, hydrogen and nitrogen) were performed using a Perkin-Elmer 2400C elemental analyzer. FT-IR spectra were obtained on a Perkin Elmer spectrometer (Spectrum Two) with the samples by using the attenuated total reflectance (ATR) technique. Powder X-ray diffraction (PXRD) patterns of the samples were recorded on a Bruker D-8 Advance instrument operated at 40 kV and 40 mA using Cu Kα (λ = 1.5406 Å) radiation. A Perkin-Elmer LS-45 fluorometer was used to carry out the fluorescence titration experiments. Vapor sensing experiments were carried out with Perkin-Elmer LS-55 fluorometer.

2.2. Synthesis of $[Cd(3\text{-bpd})(N(CN)_2)_2]_n$ (**1**)

An aqueous solution (4.0 mL) of sodium dicyanamide (2.0 mmol, 0.178 g) was added to a methanolic solution (4.0 mL) of 1,2-bis-(pyridine-3-ylmethelyne)hydrazine (3-bpd) (1.0 mmol, 0.210 g) taken in a beaker and stirred for 30 min to mix well. $Cd(NO_3)_2{\cdot}4H_2O$ (1.0 mmol, 0.308 g) was dissolved in 4.0 mL of water in a test tube. Then the previously prepared mixed ligand solution was slowly and carefully layered with the aqueous $Cd(NO_3)_2$ solution using 5.0 mL of a 1:1 *v/v* water/methanol mixture as buffer. The yellow needle-shaped crystals suitable for single crystal X-ray analysis were obtained after a few days. The crystals were collected and washed with a methanol–water mixture and dried under vacuum. (Yield = 76%.) *Anal.* Calc. for $C_{16}H_{10}N_{10}Cd$: C, 42.22; H, 2.20; N, 30.79. Found: C, 42.28; H, 2.29; N, 30.71%.

2.3. Theoretical calculations

All the theoretical calculations were performed with the help of Gaussian 03 program [26]. The optimized geometries and the orbital diagram were obtained from B3LYP hybrid function with 6-31G basis set for H, C, N and O atoms.

2.4. Detection limit calculation

The detection limit was calculated by using the following empirical equation,

$$\text{Limit of detection (LOD)} = 3\sigma/k$$

(where σ: standard deviation and k: slope).

For **1** standard deviation was calculated from fluorescence spectroscopic measurements. The measurement was repeated five times, and then standard deviation (σ) was calculated. Gradual quenching of the emission intensity of the MOFs at 430 nm during fluorometric titration with TNP was plotted against the concentration of epNACs (TNP). The slope (k) was derived from this plot.

2.5. Crystallographic data collection and refinement

A suitable yellow colored block shaped single crystal of complex **1** was mounted on the tip of a glass fiber with the help of commercially available super glue. X-ray single crystal data were collected at room temperature using a Bruker APEX II diffractometer, equipped with a fine-focus, sealed tube X-ray source with graphite monochromated Mo Kα radiation (λ = 0.71073 Å). The data were integrated using a SAINT program [27] and the absorption correction was made with SADABS [27]. The structure was solved by SHELXT [28] using direct methods and refined by full matrix least-squares on F^2 using SHELXL-2014/7 [29] with anisotropic displacement parameters for all non-hydrogen atoms. All the hydrogen atoms were fixed geometrically and placed in ideal positions. The crystal selected for the X-ray diffraction experiment was refined as a merohedral twin with an almost equal contribution of both components of 0.50(5). Of the possible space groups based on the systematic extinctions (*C*2, *Cm*, *C*2/*m*) the *C*2 space group was selected due to the non-centrosymmetric intensity statistics, the successful solution and refinement of the structure, and the lack of disorder affecting the dicyanamido anion imposed by the presence of the mirror plane in *Cm* and *C*2/*m*. Data collection and structure refinement parameters are given in Table 1.

3. Results and discussion

3.1. Description of crystal structure of complex 1

An ORTEP diagram of the single asymmetric unit of **1** is shown in Fig. 1. Selected bond lengths and bond angles of it are listed in Table 2. The asymmetric unit consists of Cd^{2+} ion, the organic ligand 3-bpd, and dicyanamide ion in the stoichiometric molar ratio of 0.5:0.5:1. The cadmium atom lies on a twofold axis and displays an almost regular octahedral coordination geometry provided by the nitrogen atoms of two crystallographically independent 3-bpd ligands and four dicyanamide ions The Cd–N bond distances, trans- and cis-bond angles fall in the ranges 2.317(12)–2.376(10) Å, 177.5(6)–180.0(7)°, 85.50(13)–97.0(6)°, respectively.

Table 1
Crystal data for **1**.

Formula	$C_{16}H_{10}CdN_{10}$
Formula weight	454.74
Crystal system	monoclinic
Space group	*C*2
a (Å)	15.594(2)
b (Å)	7.0695(9)
c (Å)	9.5798(12)
α (°)	90
β (°)	125.4951(14)
γ (°)	90
V (Å^3)	859.86(19)
Z	2
D_{calc} (g cm^{-3})	1.756
μ (mm^{-1})	1.295
F(000)	448
T (K)	294(2)
θ (°)	2.61–27.50
Reflections collected	5615
Unique reflections	1980
Reflections ($I > 2\sigma(I)$)	1980
R_{int}	0.02
Goodness-of-fit (GOF) on (F^2)	1.167
R_1 ($I > 2\sigma(I)$)[a]	0.0195
wR_2[a]	0.0517
Δρ maximum/minimum/e Å^{-3}	−0.30, 0.83

[a] $R_1 = \Sigma||F_o| - |F_c||/\Sigma|F_o|$, $wR_2 = [\Sigma(w(F_o^2 - F_c^2)^2)/\Sigma w(F_o^2)^2]^{1/2}$.

The 3-bpd ligand is nearly planar (the dihedral angle between the pyridine rings is 2.2(7)°) and acts as a bridge between the adjacent metal centers through the pyridine N atoms. The dicyanamide ions adopt a μ1, 5 bridging mode resulting in the formation of tetranuclear twenty-four-membered metallacycles connected into polymeric undulated layers parallel to the *ab* plane, which are further linked by the bridging role of the 3-bpd ligands into a three-dimensional network (Fig. 2).

3.2. Powder X-ray diffraction study

To check the purity of bulk material, powder X-ray diffraction (PXRD) analysis has been performed on bulk material of complex **1**. It has been observed that the peak position obtained from PXRD pattern of bulk matches well with the simulated PXRD pattern obtained from single crystal X-ray diffraction data (Fig. s1).

3.3. Nitroaromatic explosives detections

The photoluminescence studies of complex **1** have been performed with the MOF dispersed in acetonitrile at room temperature. **1** displays an emission peak at 430 nm when it is excited at 340 nm with high intensity. As Cd^{2+} possesses d^{10} electronic configuration, it is very difficult to be either oxidized or reduced [30,31]. Thus, its emission peak could not be interpreted as an MLCT (metal-to-ligand charge transfer) or an LMCT (ligand-to-metal transfer) [32]. This peak may be assigned to an intraligand ($\pi^* \rightarrow n$ or $\pi^* \rightarrow \pi$) emission [33,34]. In addition to this, complexation of the ligand with the metal center may increase the rigidity of the system reducing thereby nonradiative decay [35–37].

As this MOF has shown high emission intensity, this property may be explored in some practical applications. Thus, we have next tried to explore its potential as sensor for the detection of different nitroaromatic compounds. The sensing property of MOF with 2,6-DNT (2,6-dinitro toluene), NB (nitro benzene), 4-NBA (4-nitro benzoic acid), 1,3-DNB (1,3-dinitro benzene), 3,4-DNT (3,4-dinitro toluene), TNT (2,4,6-tri nitro toluene) and TNP with 10^{-4} M concentration has been investigated. To check the detection ability of the MOF, nitroaromatic compounds in deionized water have been gradually added with gradual increasing concentration (1 mg/10 mL) to MOF dispersed in acetonitrile and the emission intensity at 430 nm has been monitored. The emission intensity of the **1** is quenched to great extent in the presence of TNP whereas

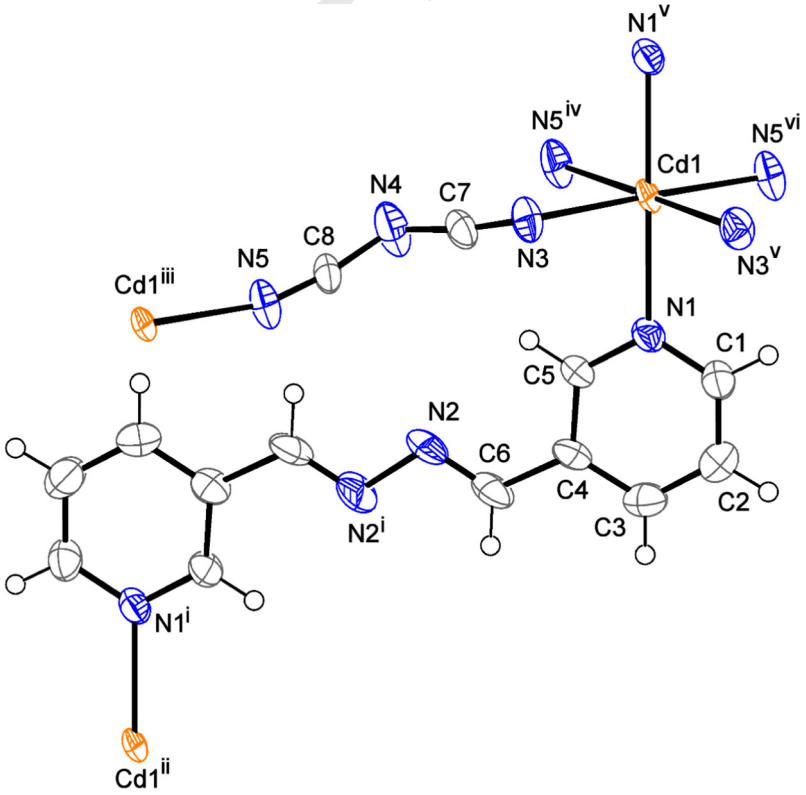

Fig. 1. The asymmetric unit of **1** with displacement ellipsoids drawn at the 50% probability level. Symmetry codes: (i) 1 − *x*, *y*, 1 − *z*; (ii) 1 + *x*, *y*, 1 + *z*; (iii) 1/2 + *x*, −1/2 + *y*, *z*; (iv) 1/2 − *x*, 1/2 + *y*, −*z*; (v) −*x*, *y*, −*z*; (vi) −1/2 + *x*, 1/2 + *y*, *z*.

Table 2
Selected bond lengths (Å) and selected bond angles (°) of complex **1**.

Cd1–N1	2.327(2)
Cd1–N3	2.376(10)
Cd1–N5^{iv}	2.317(12)
N5^{iv}–Cd1–N5^{vi}	97.0(6)
N5^{iv}–Cd1–N1^{v}	89.5(4)
N5^{vi}–Cd1–N1^{v}	90.6(4)
N5^{iv}–Cd1–N1	90.5(4)
N5^{vi}–Cd1–N1	89.5(4)
N1^{v}–Cd1–N1	180.0(7)
N5^{iv}–Cd1–N3	85.50(13)
N5^{vi}–Cd1–N3	177.5(6)
N1^{v}–Cd1–N3	90.0(4)
N1–Cd1–N3	90.0(4)
N5^{iv}–Cd1–N3^{v}	177.5(6)
N5^{vi}–Cd1–N3^{v}	85.50(13)
N1^{v}–Cd1–N3^{v}	90.0(4)
N1–Cd1–N3^{v}	90.0(4)
N3–Cd1–N3^{v}	92.1(6)
C5–N1–Cd1	120.01(18)
C1–N1–Cd1	122.2(2)
C7–N3–Cd1	121.1(6)
C8–N5^{vi}–Cd1	152.0(10)

Symmetry codes: (iv) 1/2 − *x*, 1/2 + *y*, −*z*; (v) −*x*, *y*, −*z*; (vi) −1/2 + *x*, 1/2 + *y*, *z*.

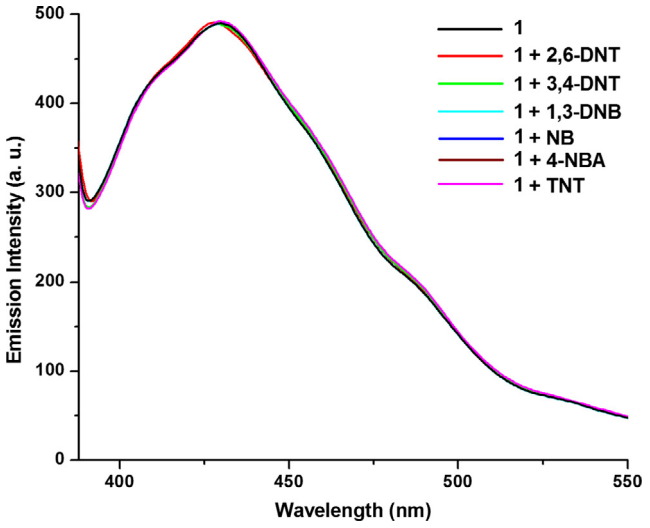

Fig. 3. Fluorescence response of **1** towards epNACs [upon addition of 0–300 μL of epNAC solution (conc. 10^{-4} M)].

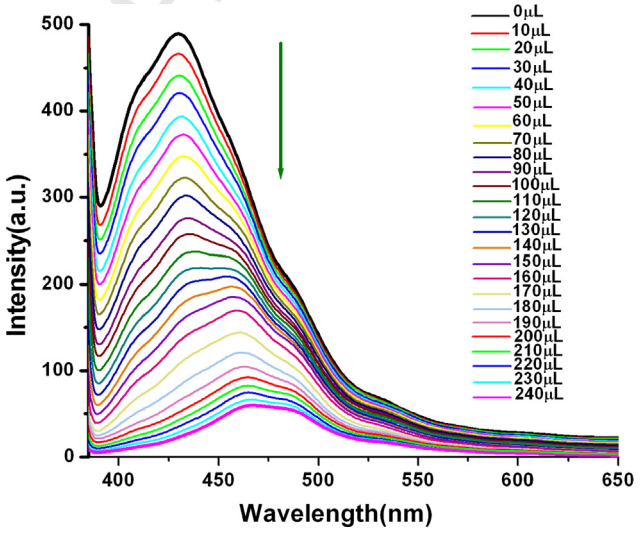

Fig. 4. Quenching in emission intensity of **1** upon gradual addition (0–240 μL) of TNP solution (10^{-4} M).

the intensity remains almost unperturbed with other epNACs. In this connection, it could be mentioned that water didn't show any influence on the initial fluorescence intensity of MOFs dispersed in MeCN (Fig. s5). Other than TNP epNACs like 4-NBA, 2,6-DNT, NB, 1,3-DNB, 3,4-DNT and TNT do not show any appreciable influence in MOFs emission (Fig. 3).

As quenching of emission intensity of **1** occurs in the presence of TNP, we have performed a titration experiment (Fig. 4). It is evident from the figure that the emission intensity of the MOF is quenched severely by its presence. To perform the titration, an aqueous solution of TNP (10^{-4} M) was gradually added to **1** dispersed in acetonitrile (1 mg/10 mL). ~95.0% of emission intensity of **1** is quenched in the presence of 240 μL of TNP.

The sensing ability of **1** towards TNP in solution encourages us to explore the emission quenching experiment in the presence of TNP vapor. The emission spectra of **1** have been recorded on a quartz glass slide before and after its exposure to equilibrated vapor of TNP over a period of specific time interval (0, 2, 5, 10, 15 min, Fig. 5). After 2 min of its exposure to TNP vapor, appreciable quenching in emission intensity of the MOF has been noticed.

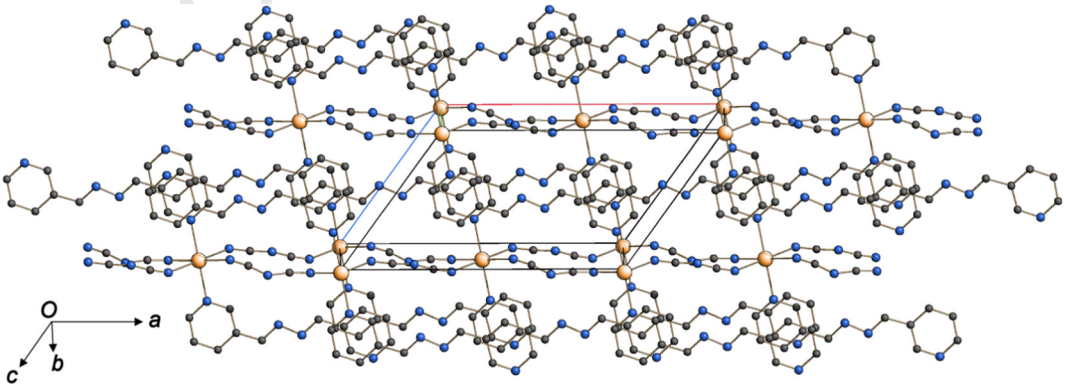

Fig. 2. Crystal packing of **1** showing the formation of a polymeric three-dimensional network. Hydrogen atoms are omitted for clarity.

Please cite this article in press as: S. Halder et al., Polyhedron (2016), http://dx.doi.org/10.1016/j.poly.2016.11.039

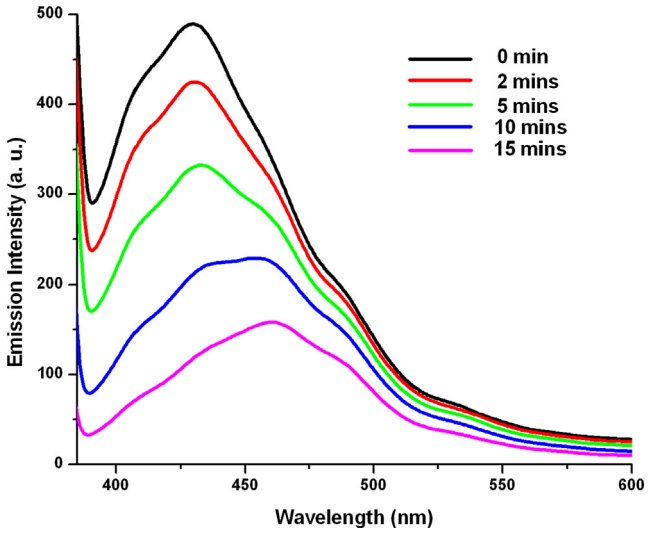

Fig. 5. Emission spectra of **1** upon exposure to TNP vapor after certain time interval.

3.4. Insight into the TNP sensing mechanism

There may be different possible explanations behind the fluorescence quenching of **1** in the presence of TNP. Among them photoinduced electron transfer (PET) and resonance energy transfer (RET) are extremely well known. Generally, in PET easy transfer of electron in the excited state takes place, which ultimately results in fluorescence quenching. On the other hand, RET involves the transfer of energy from an electronically excited donor chromophore to the acceptor. In large MOFs such as **1**, one can treat the valence and conduction band similarly as molecular orbitals (MOs) [38]. Usually it has been found that the LUMOs of epNACs lie lower in energy in comparison to the conduction bands of MOFs, which influence the transfer of electron density from the electron-rich MOFs to the electron-deficient epNACs and as a result, quenching in the emission intensity of MOFs may be observed. The HOMO and LUMO energies along with their orbital diagrams of these epNACs have been obtained from density functional theory (DFT) calculations. The HOMO–LUMO energy level diagram for some selected epNACs is represented in Fig. 5 and the values of their respective energies (in eV) are tabulated (Table 3). The DFT calculations have been carried out using the Gaussian 03 program [26] and geometry optimizations have been performed with B3LYP hybrid function with 6-31G basis set for H, C, N and O atoms.

As shown in Fig. 6, it can be clearly seen that among the several epNACs used so far, the LUMO energy of TNP is the lowest and its HOMO–LUMO energy gap is also minimum. Alternatively it can be said that the LUMO of TNP lies in a favorable energy state to the conduction band of **1** which may favor maximum electron transfer, resulting in quenching of emission intensity of the MOF. One can determine whether the quenching in emission intensity relies on electron transfer by adding an electron-rich aromatic compound (e.g. toluene) to recover the lost emission. If the fluorescence quenching, mainly, involves the electron transfer process, then addition of electron-rich analytes can recover the lost emission [39], as this can facilitate the transfer of the excited electron from the high-energy LUMO of the analyte to the conduction band of MOF. This electron transfer can enhance the radiative band gap emission and finally yield a recovery in fluorescence. Accordingly, when toluene is added into the system containing TNP and the MOF (i.e. emission-quenched solution), there is no recovery in emission. This fact establishes that the photo induced electron transfer process is not the operating mechanism in the present work.

The Stern–Volmer (SV) plot for **1** (Fig. 7) strongly implies the existence of resonance energy transfer (RET) mechanism between TNP and **1** in the present case $[(I_o/I) = K_{sv}(A) + 1$; where I_o = initial fluorescence intensity of **1** and I = fluorescence intensity in the presence of epNACs for **1**, $\{A\}$ = molar concentration of the nitroaromatic compounds and K_{sv} = quenching constant $(M^{-1})]$. The non linear feature in the S–V plot of **1** indicates that the quenching process is based on self-adsorption or an energy transfer pathway. The modified SV equation can be used in this regard. The equation, $\log(I_o/I - 1) = \log K_{sv} + n\log[Q]$, can be used for the determination of the quenching constant value, where n is the number of association

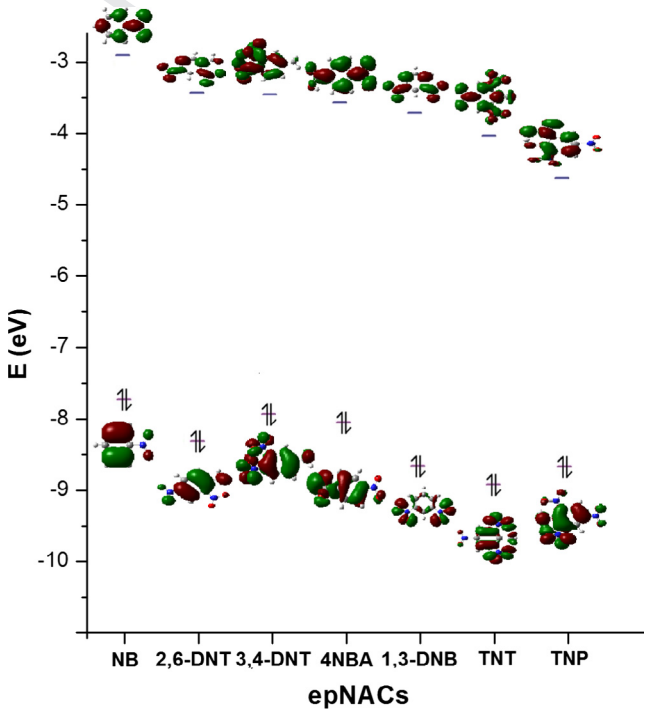

Fig. 6. HOMO–LUMO energy level diagram of some epNACs (violet: LUMO energy level and magenta: HOMO energy level). (Color online).

Table 3
HOMO–LUMO energy levels of different explosives obtained from theoretical calculations.

epNACs	LUMO energy (eV)	HOMO energy (eV)	HOMO–LUMO energy gap (eV)
NB	−2.9089	−7.7484	4.8395
2,6-DNT	−3.4684	−8.3465	4.8781
3,4-DNT	−3.4782	−7.9795	4.5013
4-NBA	−3.5818	−8.1245	4.5427
1,3-DNB	−3.6379	−8.6121	4.9742
TNT	−4.0295	−8.7427	4.7132
TNP	−4.5225	−8.5892	4.0667

Please cite this article in press as: S. Halder et al., Polyhedron (2016), http://dx.doi.org/10.1016/j.poly.2016.11.039

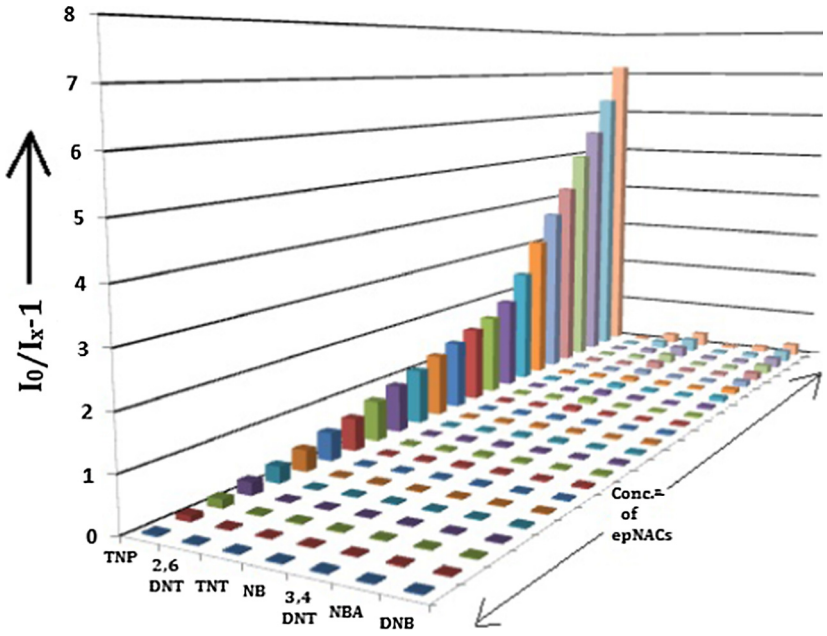

Fig. 7. Stern–Volmer (SV) plot of **1** with epNACs.

points between **1** and epNACs, I_o is initial fluorescence intensity and I is fluorescence intensity of **1** in the presence of epNACs, [Q] is the molar concentration of epNACs and K_{sv} is the quenching constant (M^{-1}). Mathematically, the intercept of the $\log(I_o/I-1)$ versus log [Q] plot gives the K_{sv}. The calculated K_{sv} value is found to be $7.16 \times 10^4\ M^{-1}$. The quenching constant value is larger with some recently published values e.g. $[Cd_3(TPT)_2(DMF)_2]\cdot(H_2O)_{0.5}$ ($6.56 \times 10^4\ M^{-1}$) [40]; $[Cd_5(TCA)_4(H_2O)_2]$ ($6.56 \times 10^4\ M^{-1}$) [41]; $\{[Cd_4(L)_2(L_2)_3(H_2O)_2](8DMF)(8H_2O)\}_n$ ($3.89 \times 10^4\ M^{-1}$) [42]; $[Cd_4(\mu_3\text{-}O)(TTHA)(H_2O)_2]\cdot 3H2O$ ($3.83 \times 10^4\ M^{-1}$) [43]; $\{[Eu_2(TDC)_3(CH_3OH)_2]\cdot CH_3OH\}$ ($1.6 \times 10^4\ M^{-1}$) [44]; $[Zn_8(ad)_4(BPDC)_6\text{-}O\cdot 2Me_2NH_2]\cdot G$ (G = DMF and water) ($4.6 \times 10^4\ M^{-1}$) [45]. The limit of detection for **1** has been found to be 6×10^{-5} M.

The resonance energy can be transferred easily from the excited fluorophore to the electron deficient TNP if there is suitable overlapping between the absorption band of TNP with the emission band of the fluorophore **1**. The RET process, mainly, depend on the extent of overlap of the absorption spectrum of TNP with the emission spectrum of the MOF. It is evident from Fig. 8 that among the investigated epNACs the maximum overlap has been observed between the emission spectrum of **1** and the absorption spectrum of TNP. For other epNACs the extent of overlap is considerably less. Therefore, it may be concluded that resonance energy transfer is responsible for the speedy and selective emission quenching of **1** with high sensitivity towards TNP.

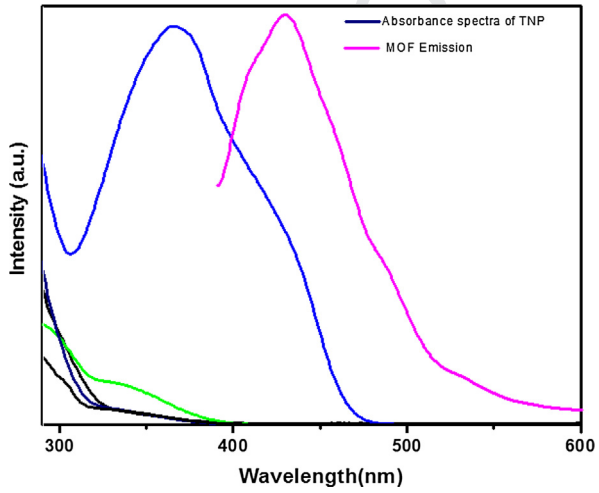

Fig. 8. Overlap of epNACs absorption spectra with fluorescence spectra of of MOF.

Nitrophenols are acidic in nature. We examine whether these compounds including trinitrophenol are able to coordinate with the metal center under the experimental conditions when 3-bpd or thiocyanato moieties may vacate coordination site for the nitrophenol. It has been found that phenolic oxygen atoms are unable to bind with the cadmium atom as revealed by the IR spectral studies. FT-IR spectrum was recorded with the recovered compound **1** after its treatment with TNP. Comparison of FT-IR spectra of **1** and **1** after recovery shows that they are exactly identical (Fig. s2). This indicates that nitrophenols are unable to replace the existing ligands around the metal center. When we repeat the experiment with 4-NBA instead of TNP, results remain same i.e. 4-NBA is also unable to coordinate with Cd center. Moreover, oxygen atom is hard compared to nitrogen or sulfur and Cd(II) is a soft center. Thus, it is expected the coordination of Cd and N or S will be stronger compared to Cd and O.

3.5. Selectivity of sensing TNP in the presence of other epNACs

It is evident from the previous studies that **1** has high selectivity towards TNP compared to other epNACs. Therefore, it could be interesting to explore the selectivity of **1** towards TNP in the presence of other epNACs. The selectivity has been tested by the following steps: (i) first of all, the emission intensity of **1** in a highly dispersed state in MeCN has been found out; this value is about 490 a.u. (ii) An aqueous solution of 2,6-DNT (10^{-1} M) is then added to the highly dispersed solution of **1** in MeCN, and the corresponding emission is measured. Addition of 2,6-DNT shows a negligible change in the emission intensity of **1**. A similar trend has been observed also for the other epNACs (3,4-DNT, 1,3-DNB, 4-NBA, NB, TNT). In conclusion it can be said that all the epNACs except TNP do not have any noticeable effect on the emission intensity of **1**. (iii) The selectivity has been finally verified by addition of an aqueous solution of TNP to solutions of epNACs

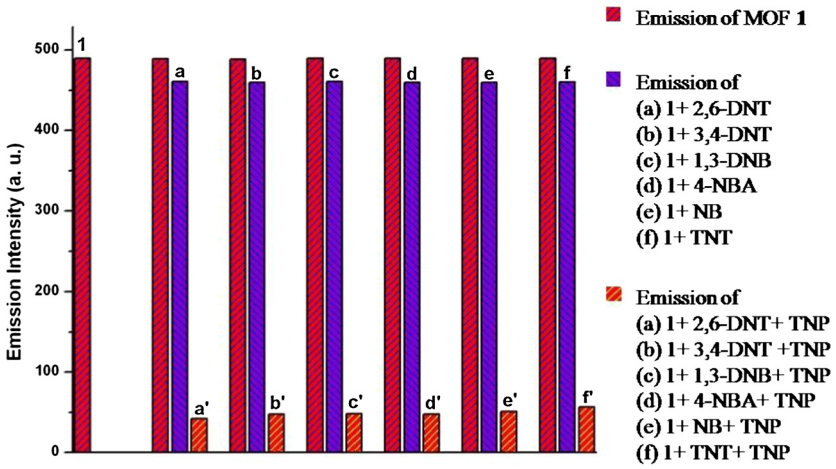

Fig. 9. Selectivity of **1** for TNP in the presence of other epNACs.

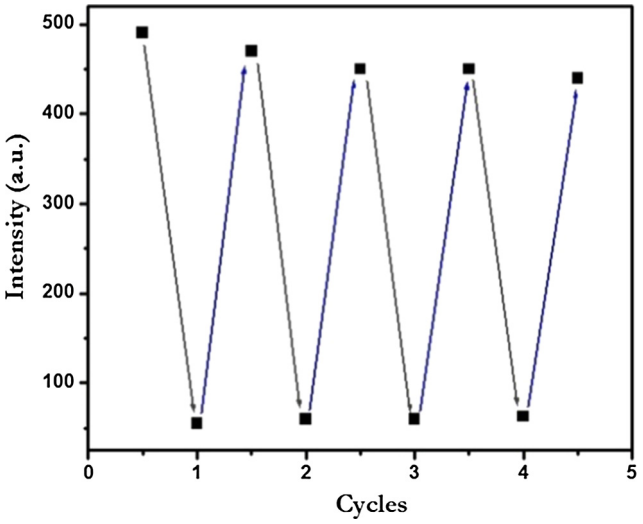

Fig. 10. The recyclability test of **1** in MeCN. The up square dots represent the initial luminescent intensity and the down one represents the intensity upon addition of TNP (gray color line represents fluorescence quenching and blue color line represents recyclability). (Color online.)

(2,6-DNT, NB, 4-NBA, 1,3-DNB, 3,4-DNT, and TNT) containing **1**. Addition of TNP results in appreciable quenching in the emission intensity (from 490 a.u. to ca. 25 a.u.). These results show the selective sensitivity of **1** for TNP even in the presence of several other epNACs (Fig. 9).

3.6. Recyclability and recovery experiments

Fig. 10 shows that the fluorescence intensity remains almost same after four cycles of TNP sensing compared to the MOF's initial state. This result suggests that the material have high stability and recyclability for TNP detection. The recyclability of MOF is comparable with recent reports of MOFs in related area [40,46].

Complex **1** is insoluble in common solvents including water. It is recovered by simple filtration. There is no detectable amount of Cd in the solution after recovery of the complex. If **1** were dissociated in aqueous medium, then free 3-bpd should have been found the medium. It has distinct fluorescence peak and spectrum. But we did not get any other peak. Dissociation of the MOF in water would also produce Cd^{2+} ion. Interaction of Cd^{2+} with sulfide ion in slightly acidic or basic medium produces precipitation of CdS which is yellow in color [47]. Addition of sufficient amount of

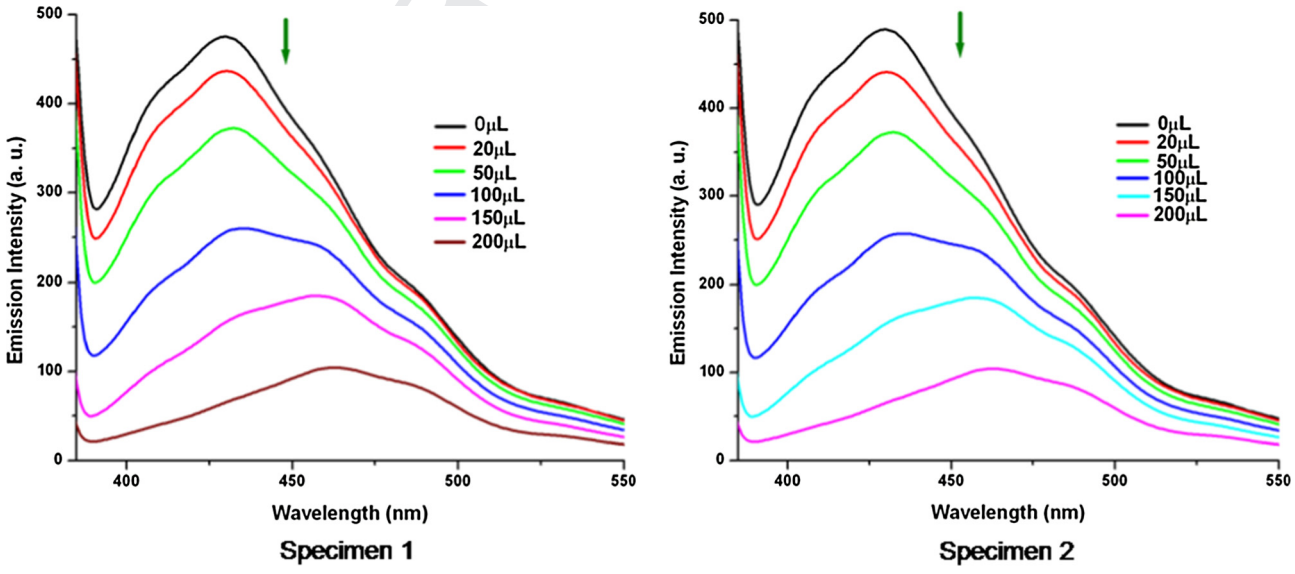

Fig. 11. Quenching in emission intensity of **1** upon gradual addition of TNP solution in river water.

Please cite this article in press as: S. Halder et al., Polyhedron (2016), http://dx.doi.org/10.1016/j.poly.2016.11.039

sodium sulfide to the filtrate after recovery of the complex does not produce any precipitation confirming no dissociation of **1** in water.

3.7. Detection of TNP in river water

Apart from being a highly explosive material, TNP is also a toxic pollutant. When it enters into mammalian metabolic system it is converted to mutagenic picramic acid. Municipality water is generally supplied from river, lake, sea, ocean after its purification. Water from river Ganga is used in Kolkata, India. Contamination of TNP in this river water is possible due to the presence of the industrial wastes. This kind of contamination may create severe health hazard. Therefore, selective detection of TNP is necessary not only in deionized water but also in water obtained from natural resources. For this purpose different river water specimens have been collected from Ganga at Diamond Harbour (60 km downstream from Kolkata, specimen 1) and Barrackpore (30 km upstream from Kolkata, specimen 2). To ensure the effectiveness of the MOF, different sets of TNP solution (1 mM) have been prepared separately with the water (specimen 1 and specimen 2) and its influence on the MOF dispersed acetonitrile solution has been monitored. A highly appreciable quenching of emission intensity has been observed in each case (Fig. 11). It should be mentioned here that water sample without TNP (black line) showed no influence on emission spectrum of **1**. Thus, it can be said that irrespective of the source of water, the emission intensity of **1** is always quenched in the presence of TNP. Therefore, **1** can be treated as a universal sensor for TNP.

4. Conclusion

In this article, synthesis and characterization of a new Cd-based MOF $[Cd(3\text{-bpd})(N(CN)_2)_2]_n$ have been possible and the fluorescence quenching of this MOF in the presence of TNP extensively studied. It has been found that the TNP sensing capability of the MOF is highly selective even in the presence of other nitroaromatic compounds. Apart from studying its sensitivity towards TNP in deionized water, it has been observed that its sensitivity remains intact in river water. This eventually established this Cd-based MOF as a universal sensor for TNP-like organic explosives and mutagenic pollutants.

Acknowledgments

PR thanks DST, New Delhi for financial supports. SH thanks CSIR, New Delhi for his fellowship. PB is thankful to CSIR-XIIth five year plan project (CSIR-Supra institutional grant: ESC 0203/9). PG is thankful to DST (GAP-183112) for his fellowship. Authors acknowledge DST Special Grant to the Department of Chemistry, Jadavpur University in the International Year of Chemistry 2011.

Appendix A. Supplementary data

CCDC 1501522 contains the supplementary crystallographic data for **1**. These data can be obtained free of charge via http://www.ccdc.cam.ac.uk/conts/retrieving.html, or from the Cambridge Crystallographic Data Centre, 12 Union Road, Cambridge CB2 1EZ, UK; fax: (+44) 1223-336-033; or e-mail: deposit@ccdc.cam.ac.uk. Supplementary data associated with this article can be found, in the online version, at http://dx.doi.org/10.1016/j.poly.2016.11.039.

References

[1] (a) H.C.J. Zhou, S. Kitagawa, Chem. Soc. Rev. 43 (2014) 5415;
(b) A.J. Lan, K.H. Li, H.H. Wu, D.H. Olson, T.J. Emge, W. Ki, M.C. Hong, J. Li, Angew. Chem., Int. Ed. 48 (2009) 2334;
(c) S. Pramanik, C. Zheng, X. Zhang, T.J. Emge, J. Li, J. Am. Chem. Soc. 133 (2011) 4153;
(d) A.J. Lan, K.H. Li, H.H. Wu, L.Z. Kong, N. Nijem, D.H. Olson, T.J. Emge, Y.J. Chabal, D.C. Langreth, M.C. Hong, J. Li, Inorg. Chem. 48 (2009) 7165;
(e) D. Banerjee, Z. Hu, J. Li, Dalton Trans. 43 (2014) 10668.
[2] (a) J.A. Mason, M. Veenstra, J.R. Long, Chem. Sci. 5 (2014) 32;
(b) S. Chaemchuen, N.A. Kabir, K. Zhou, F. Verpoort, Chem. Soc. Rev. 42 (2013) 9304;
(c) J. Liu, P.K. Thallapally, B.P. McGrail, D.R. Brown, J. Liu, Chem. Soc. Rev. 41 (2012) 2308;
(d) K. Sumida, D.L. Rogow, J.A. Mason, T.M. McDonald, E.D. Bloch, Z.R. Herm, T. H. Bae, J.R. Long, Chem. Rev. 112 (2012) 724;
(e) J.R. Li, J. Sculley, H.C. Zhou, Chem. Rev. 112 (2012) 869;
(f) E. Barea, C. Montoro, J.A.R. Navarro, Chem. Soc. Rev. 43 (2014) 5419.
[3] (a) M. Eddaoudi, D.F. Sava, J.F. Eubank, K. Adil, V. Guillerm, Chem. Soc. Rev. 44 (2015) 228;
(b) J. Liu, L. Chen, H. Cui, J. Zhang, L. Zhang, C.-Y. Su, Chem. Soc. Rev. 43 (2014) 6011;
(c) T. Zhang, W. Lin, Chem. Soc. Rev. 43 (2014) 5982;
(d) A. Dhakshinamoorthy, H. Garcia, Chem. Soc. Rev. 43 (2014) 5750;
(e) S.H.A.M. Leenders, R. Gramage-Doria, B.D. Bruin, J.N.H. Reek, Chem. Soc. Rev. 44 (2015) 433.
[4] (a) S. Halder, A. Layek, K. Ghosh, C. Rizzoli, P.P. Ray, P. Roy, Dalton Trans. 44 (2015) 16149;
(b) V. Stavila, A.A. Talin, M.D. Allendorf, Chem. Soc. Rev. 43 (2014) 5994.
[5] L.E. Kreno, K. Leong, O.K. Farha, M. Allendorf, R.P. Van Duyne, J.T. Hupp, Chem. Rev. 112 (2012) 1105.
[6] (a) P. Mahata, C.M. Draznieks, P. Roy, S. Natarajan, Cryst. Growth Des. 13 (2013) 155;
(b) P. Mahata, S. Natarajan, P. Panissod, M. Drillon, J. Am. Chem. Soc. 131 (2009) 10140.
[7] S.S. Nagarkar, B. Joarder, A.K. Chaudhari, S. Mukherjee, S.K. Ghosh, Angew. Chem., Int. Ed. 52 (2013) 2953.
[8] P. Ghosh, S.K. Saha, A.R. Chowdhury, P. Banerjee, Eur. J. Inorg. Chem. 17 (2015) 2851;
(b) P. Ghosh, P. Banerjee, Phys. Chem. Chem. Phys. 18 (2016) 22805.
[9] G. He, H. Peng, T. Liu, M. Yang, Y. Zhang, Y. Fang, J. Mater. Chem. 19 (2009) 7347.
[10] S.S. Nagarkar, A.V. Desai, S.K. Ghosh, Chem. Commun. 50 (2014) 8915.
[11] J. Ye, L. Zhao, R.F. Bogale, Y. Gao, X. Wang, X. Qian, S. Guo, J. Zhao, G. Ning, Chem. Eur. J. 21 (2015) 2029.
[12] K.M. Wollin, H.H. Dieter, Arch. Environ. Contam. Toxicol. 49 (2005) 18.
[13] J. Rocha, L.D. Carlos, F.A.A. Paz, D. Ananias, Chem. Soc. Rev. 40 (2011) 926.
[14] J.C.G. Bunzli, C. Piguet, Chem. Rev. 102 (2002) 1897.
[15] M.D. Allendorf, C.A. Bauer, R.K. Bhakta, R.J.T. Houk, Chem. Soc. Rev. 38 (2009) 1330.
[16] J. Heine, K. Muller-Buschbaum, Chem. Soc. Rev. 42 (2013) 9232.
[17] M.S. Wang, S.P. Guo, Y. Li, L.Z. Cai, J.P. Zou, G. Xu, W.W. Zhou, F.K. Zheng, G.C. Guo, J. Am. Chem. Soc. 131 (2009) 13572.
[18] H.M. He, F.X. Sun, T. Borjigin, N. Zhao, G.S. Zhu, Dalton Trans. 43 (2014) 3716.
[19] B. Gole, A.K. Bar, P.S. Mukherjee, Chem. Eur. J. 20 (2014) 2276.
[20] B. Gole, A.K. Bar, P.S. Mukherjee, Chem. Eur. J. 20 (2014) 13321.
[21] S. Sanda, S. Parshamoni, S. Biswas, S. Konar, Chem. Commun. 51 (2015) 6576.
[22] X.D. Zhu, Y. Li, W.X. Zhou, R.M. Liu, Y.J. Ding, J. Lü, D.M. Proserpio, CrystEngComm 18 (2016) 4530.
[23] Z.Q. Shi, Z.J. Guoa, H.G. Zheng, Chem. Commun. 51 (2015) 8300.
[24] (a) Y.B. Dong, M.D. Smith, R.C. Layland, H.C. Zur Loye, Chem. Mater. 12 (2000) 1156;
(b) A. Das, B. Bhattacharya, D.K. Maity, A. Halder, D. Ghoshal, Polyhedron 117 (2016) 585;
(c) D.K. Maity, B. Bhattacharya, A. Halder, D. Ghoshal, Dalton Trans. 44 (2015) 20999;
(d) D.K. Maity, B. Bhattacharya, R. Mondal, D. Ghoshal, CrystEngComm 16 (2014) 8896.
[25] R.C. Dorey, W.R. Carper, J. Chem. Eng. Data 29 (1984) 93.
[26] M.J. Frisch, G.W. Trucks, H.B. Schlegel, G.E. Scuseria, M.A. Robb, J.R. Cheeseman, J.A. Montgomery Jr., T. Vreven, K.N. Kudin, J.C. Burant, J.M. Millam, S.S. Iyengar, J. Tomasi, V. Barone, B. Mennucci, M. Cossi, G. Scalmani, N. Rega, G.A. Petersson, H. Nakatsuji, M. Hada, M. Ehara, K. Toyota, R. Fukuda, J. Hasegawa, M. Ishida, T. Nakajima, Y. Honda, O. Kitao, H. Nakai, M. Klene, X. Li, J.E. Knox, H. P. Hratchian, J.B. Cross, V. Bakken, C. Adamo, J. Jaramillo, R. Gomperts, R.E. Stratmann, O. Yazyev, A.J. Austin, R. Cammi, C. Pomelli, J.W. Ochterski, P.Y. Ayala, K. Morokuma, G.A. Voth, P. Salvador, J.J. Dannenberg, V.G. Zakrzewski, S. Dapprich, A.D. Daniels, M.C. Strain, O. Farkas, D.K. Malick, A.D. Rabuck, K. Raghavachari, J.B. Foresman, J.V. Ortiz, Q. Cui, A.G. Baboul, S. Clifford, J. Cioslowski, B.B. Stefanov, G. Liu, A. Liashenko, P. Piskorz, I. Komaromi, R.L. Martin, D.J. Fox, T. Keith, M.A. Al-Laham, C.Y. Peng, A. Nanayakkara, M. Challacombe, P.M.W. Gill, B. Johnson, W. Chen, M.W. Wong, C. Gonzalez, J.A. Pople, Gaussian 03 (Revision C.02), Gaussian Inc., Wallingford, CT, 2004.
[27] APEX-II, SAINT and SADABS, Bruker AXS Inc., Madison, WI, 2008.
[28] G.M. Sheldrick, Acta Crystallogr. A71 (2015) 3.
[29] G.M. Sheldrick, Acta Crystallogr. C71 (2015) 3.
[30] Y.J. Cui, Y.F. Yue, G.D. Qian, B.L. Chen, Chem. Rev. 112 (2012) 1126.
[31] C. Vijayakumar, G. Tobin, W. Schmitt, M.J. Kim, M. Takeuchi, Chem. Commun. 46 (2010) 874.

[32] M.D. Allendorf, C.A. Bauer, R.K. Bhaktaa, R.J.T. Houka, Chem. Soc. Rev. 38 (2009) 1330.
[33] F.J. Liu, D. Sun, H.J. Hao, R.B. Huang, L.S. Zheng, Cryst. Growth Des. 12 (2012) 354.
[34] D. Sun, H.R. Xu, C.F. Yang, Z.H. Wei, N. Zhang, R.B. Huang, L.S. Zheng, Cryst. Growth Des. 10 (2010) 4642.
[35] Q.L. Zhu, C.J. Shen, C.H. Tan, T.L. Sheng, S.M. Hua, X.T. Wu, Chem. Commun. 48 (2012) 531.
[36] H.Y. Bai, J.F. Ma, J. Yang, Y.Y. Liu, H. Wu, J.C. Ma, Cryst. Growth Des. 10 (2010) 995.
[37] X.L. Wang, C. Qin, E.B. Wang, Z.M. Su, L. Xu, S.R. Batten, Chem. Commun. (2005) 4789.
[38] S.S. Nagarkar, B. Joarder, A.K. Chaudhari, S. Mukherjee, S.K. Ghosh, Angew. Chem., Int. Ed. 52 (2013) 2881.
[39] Z. Hu, B.J. Deibert, J. Li, Chem. Soc. Rev. 43 (2014) 5815.
[40] C. Zhang, L. Sun, Y. Yan, J. Li, X. Song, Y. Liu, Z. Liang, Dalton Trans. 44 (2015) 230.
[41] M. Venkateswarulu, A. Pramanik, R.R. Koner, Dalton Trans. 44 (2015) 6348.
[42] T.K. Pal, N. Chatterjee, P.K. Bharadwaj, Inorg. Chem. 55 (2016) 1741.
[43] S. Li, J. Song, J.C. Ni, Z.N. Wang, X. Gao, Z. Shi, F.Y. Baia, Y.H. Xing, RSC Adv. 6 (2016) 36000.
[44] F. Zhang, Y. Wang, T. Chu, Z. Wang, W. Li, Y. Yang, Analyst 141 (2016) 4502.
[45] B. Joarder, A.V. Desai, P. Samanta, S. Mukherjee, S.K. Ghosh, Chem. Eur. J. 21 (2015) 965.
[46] L. Sun, H. Xing, J. Xu, Z. Liang, J. Yu, R. Xu, Dalton Trans. 42 (2013) 5508.
[47] Vogel's Qualitative Inorganic Analysis, Seventh ed., Revised by G. Svehla, Pearson Education Ltd., Delhi, 2009.